

# Phenomenology of light remnant doubly charged Higgs fields in the supersymmetric left-right model

B. Dutta

*Institute of Theoretical Sciences, University of Oregon, Eugene, Oregon 97403*

R. N. Mohapatra

*Department of Physics, University of Maryland, College Park, Maryland 20742*

(Received 17 April 1998; published 10 December 1998)

It has recently been shown that in supersymmetric left-right models with automatic  $R$ -parity conservation, the theory below the  $W_R$  scale is given by the MSSM with massive neutrinos and a pair of doubly charged superfields with masses in the 100 GeV range [with or without an extra pair of heavy Higgs doublets ( $M \geq 10$  TeV) depending on the model]. In this paper we study the unification prospects for such theories and their phenomenological implications for collider experiments. We study two versions of the theory: one with supersymmetry breaking transmitted via the gauge and another where the same occurs via gravitational forces. We point out that looking at multi  $\tau$  final states can considerably constrain the parameter space of the model. [S0556-2821(98)07019-2]

PACS number(s): 12.60.Jv

## I. INTRODUCTION

Supersymmetric left-right models (SUSYLR) where the  $SU(2)_R$  gauge symmetry is broken by triplet Higgs fields with  $B-L=2$  have many attractive features: (1) they imply automatic conservation of baryon and lepton number [1], a property which makes the standard model so attractive, but is not shared by the minimal supersymmetric standard model (MSSM); (2) they provide a natural solution to the strong and weak  $CP$  problems of the MSSM [2]; (3) they yield a natural embedding of the seesaw mechanism for small neutrino masses [3] where the right-handed triplet field ( $\Delta^c$ ) that breaks the  $SU(2)_R$  symmetry also gives a heavy mass to the right-handed Majorana neutrino needed for implementing the seesaw mechanism.

In order to cancel anomalies as well as to maintain supersymmetry below the  $SU(2)_R$  scale ( $v_R$ ), one needs a pair of fields  $\Delta^c \oplus \bar{\Delta}^c$  with  $B-L = \mp 2$ , respectively. An important distinguishing characteristic of these Higgs multiplets is that they contain doubly charged Higgs bosons and Higgsinos in them which remain as physical fields subsequent to symmetry breakdown. It has recently been shown that the vacuum of the theory may or may not conserve  $R$  parity [4]. If, however, it is required that the ground state conserves  $R$  parity, one must include higher dimensional operators [2,5] or additional Higgs fields which break parity [4,7]. In this case, [7,6] the model in its simple versions, always predicts that some of the doubly charged fields, mentioned above, are massless in the absence of the higher dimensional operators (HDO). This is independent of whether the hidden sector supersymmetry breaking scale is above or below the  $W_R$  scale. In the presence of HDO's, they acquire masses of order  $\sim v_R^2/M_{Pl}$ . Since the measurement of the  $Z$  width at the CERN  $e^+e^-$  collider LEP and SLAC Linear Collider (SLC) implies that such particles must have a mass of at least 45 GeV, this puts a lower limit on the  $W_R$  scale of about  $10^{10}$  GeV or so. This result is interesting since  $W_R$  masses in

this range also lead to neutrino masses expected on the basis of current solar and atmospheric neutrino experiments. If we take the  $W_R$  mass to be close to this lower limit (say of order  $10^{10}$ – $10^{11}$  GeV), it implies the masses of the doubly charged particles in the 100 GeV range. There are two bosonic and two fermionic particles of this type. The rest of the particle spectrum below the  $W_R$  scale can be same as that of the minimal supersymmetric standard model (MSSM) with a massive neutrino or it can have an extra pair of Higgs doublets in the 10 TeV range depending on the structure of the model. It is the goal of this paper to explore the constraints on the parameters of the model and suggest tests in the  $e^+e^-$  and  $p\bar{p}$  collider.

Our main results are that for a large range of parameters in this model, the lighter stau is the lightest of the sleptons due to the renormalization group running arising from the  $\Delta^{++}\tau^-\tau^-$  coupling which is not very constrained from phenomenology. (Note that the  $\Delta^{++}$  couplings to other leptons are severely bounded by the recent PSI results on muonium-antimuonium oscillation [8].) As a result, tau lepton final states, generated from the production of the  $\Delta^{\pm\pm}$  and its fermionic part, provide a crucial signature of this class of models. For instance, we find that detection of final states of type  $\tau^-\tau^-\tau^+\tau^+\gamma\gamma$  plus missing energy or  $\tau^-\tau^-\tau^+\tau^+$  with or without missing energy in both  $p\bar{p}$  and  $e^+e^-$  collision will provide test of these models. Thus nonobservation of such signals will significantly reduce the domain of allowed parameters of this model. We point out the difference between the multi- $\tau$  signals of this model and the same type of signals that appear in the other models, e.g., conventional gauge mediated supersymmetry breaking (GMSB) type. We will show that the allowed region of parameter space is larger when we choose GMSB type of theories. We also discuss the unification prospects of this model in different SUSY breaking scenarios.

This paper is organized as follows: in Sec. II, we review the arguments leading to the existence of light doubly

TABLE I. Field content of the SUSY LR model; we assume that  $S$  is odd under parity;  $U$  and  $V$  denote the  $SU(2)_{L,R}$  transformations, respectively.

Fields	$SU(2)_L \times SU(2)_R \times U(1)_{B-L}$ representation	Group transformation
$Q$	$(2, 1, +\frac{1}{3})$	$UQ$
$Q^c$	$(1, 2, -\frac{1}{3})$	$VQ^c$
$L$	$(2, 1, -1)$	$UL$
$L^c$	$(1, 2, +1)$	$VL^c$
$\Phi_{1,2}$	$(2, 2, 0)$	$U\phi V^\dagger$
$\Delta$	$(3, 1, +2)$	$U\Delta U^\dagger$
$\bar{\Delta}$	$(3, 1, -2)$	$U\bar{\Delta} U^\dagger$
$\Delta^c$	$(1, 3, +2)$	$V\Delta^c V^\dagger$
$\bar{\Delta}^c$	$(1, 3, -2)$	$V\bar{\Delta}^c V^\dagger$
$S$	$(1, 1, 0)$	$S$

charged fields despite a high  $W_R$  scale in the context of a simple model and discuss the low energy interactions of these fields; in Sec. III we discuss gauge unification in these models; in Sec. IV, we discuss its parameter space and experimental signals in gravity mediated SUSY breaking scenario; in Sec. V, we discuss the same for the gauge mediated SUSY breaking scenarios and in Sec. VI we present our conclusion.

## II. OVERVIEW OF THE MODEL

In this section, we present a brief review of the arguments leading to the existence of the light doubly charged Higgs fields in the SUSYLR model. In order to give our arguments, we start by giving the basic features of the model, which is based on the gauge group  $SU(2)_L \times SU(2)_R \times U(1)_{B-L} \times SU(3)_c$ . In Table I, we give the particle content of the model. We will suppress the  $SU(3)_c$  indices in what follows.

The superpotential for this theory is given by (we have suppressed the generation index)

$$\begin{aligned}
W = & \mathbf{h}_q^{(i)} Q^T \tau_2 \Phi_i \tau_2 Q^c + \mathbf{h}_l^{(i)} L^T \tau_2 \Phi_i \tau_2 L^c \\
& + i(\mathbf{f} L^T \tau_2 \Delta L + \mathbf{f}_c L^c T \tau_2 \Delta^c L^c) + M_\Delta [\text{Tr}(\Delta \bar{\Delta}) \\
& + \text{Tr}(\Delta^c \bar{\Delta}^c)] + \lambda S (\Delta \bar{\Delta} - \Delta^c \bar{\Delta}^c) + \mu_S S^2 \\
& + \mu_{ij} \text{Tr}(\tau_2 \Phi_i^T \tau_2 \Phi_j) + W_{NR}, \quad (1)
\end{aligned}$$

where  $W_{NR}$  denotes nonrenormalizable terms arising from higher scale physics such as grand unified theories or Planck scale effects:

$$W_{NR} = A [\text{Tr}(\Delta^c \bar{\Delta}^c)]^2 / 2 + B \text{Tr}(\Delta^c \Delta^c) \text{Tr}(\bar{\Delta}^c \bar{\Delta}^c) / 2, \quad (2)$$

where  $A$  and  $B$  are of order  $1/M_{Planck}$ .

We will work in the vacuum which conserves  $R$  parity. The Higgs vevs then have the following pattern:

$$\langle \phi \rangle = \begin{pmatrix} \kappa & 0 \\ 0 & \kappa' \end{pmatrix}; \quad \langle \Delta^c \rangle = \begin{pmatrix} 0 & v \\ 0 & 0 \end{pmatrix}. \quad (3)$$

Similar pattern for  $\langle \bar{\Delta}^c \rangle$  is assumed.

Using Eq. (1), one can give a group theoretical argument for the existence of light doubly charged particles in the supersymmetric limit as follows. Let us first ignore the higher dimensional terms  $A$  and  $B$  as well as the leptonic couplings  $f$ . It is then clear that the superpotential has a complexified  $U(3)$  symmetry (i.e., a  $U(3)$  symmetry whose parameters are taken to be complex) that operates on the  $\Delta^c$  and  $\bar{\Delta}^c$  fields. This is due to the holomorphy of the superpotential. After one component of each of the above fields acquires vev, the resulting symmetry is the complexified  $U(2)$ . This leaves 10 massless fields. Once we bring in the D-terms and switch on the gauge fields, six of these fields become massive as a consequence of the Higgs mechanism of supersymmetric theories. That leaves four massless fields in the absence of higher dimensional terms. These are the two complex doubly charged fields. Of the two nonrenormalizable terms  $A$  and  $B$ , only the  $A$  term has the complexified  $U(3)$  symmetry. Hence, the supersymmetric contribution to the doubly charged particles will come only from the  $B$  term. It is then clear that the masses of the doubly charged fields are of order  $v_R^2/M_{Pl}$ . Requiring that these masses satisfy the  $Z$  width bound then implies that  $v_R \geq 10^{10} - 10^{11}$  GeV or so. In this paper we will assume that  $v_R$  is at the lower bound value so that the doubly charged fields are accessible to the existing collider experiments. Note incidentally that although the leptonic couplings do not respect the above mentioned symmetry, they are unimportant in determining the vacuum structure as long as  $R$  parity is conserved and, hence, they do not effect the doubly charged field masses.

Let us now give an explicit calculation of the masses of the doubly charged fields in the supersymmetric limit using the superpotential in Eq. (1). Let us write down the F-terms for the  $S$ ,  $\Delta$  and  $\Delta^c$  terms:

$$\begin{aligned}
F_S &= 2\mu_S S + \lambda(\Delta \bar{\Delta} - \Delta^c \bar{\Delta}^c), \\
F_\Delta &= (\lambda S + M_\Delta) \bar{\Delta}, \\
F_{\Delta^c} &= (-\lambda S + M_\Delta) \bar{\Delta}^c. \quad (4)
\end{aligned}$$

If the effective supersymmetry breaking scale is below the  $W_R$  scale, then these  $F$  terms must vanish. It is then clear that if we choose the  $\Delta^c$  and  $\bar{\Delta}^c$  vev's (denoted by  $v_R$  and  $\bar{v}_R$ ) to be nonvanishing (and they are equal in the supersymmetric limit), then we must have  $\langle S \rangle = M_\Delta / \lambda$ . This implies that the  $\Delta$  and  $\bar{\Delta}$  vev's vanish and the masses of these fields are of order  $2M_\Delta$ . Thus the left triplet fields decouple from the low-energy spectrum. It is then easy to see from the superpotential (in the absence of the  $A$  and  $B$  terms) that all the particles in the superfields  $\Delta^c$  and  $\bar{\Delta}^c$  are massless in the limit of exact supersymmetry. One linear combination of the neutral fields and another of singly charged fields disappear due to the Higgs mechanism. The remaining singly charged and neutral Higgs fields pick up mass of order of  $v_R$  and disappear from the low-energy spectrum.

The story of the doubly charged fields is, however, very different in this theory as has been shown in Ref. [6]. Once

supersymmetry breaking is turned on, but the higher dimensional terms  $A$  and  $B$  are excluded from the analysis, these fields acquire negative mass-squares signaling the breakdown of electric charge. This problem is cured as soon as the  $A$  and  $B$  terms are included. The doubly charged fields (all of them) then acquire masses of order  $v_R^2/M_{Pl}$  and the vacuum becomes charge conserving.

Let us now discuss the Higgs doublet spectrum of the model at low energies. At the  $W_R$  scale, one generally takes two bi-doublet fields  $\phi$ 's to make the model realistic. In order to get the MSSM at low energies, one must decouple one pair of  $H_u$  and  $H_d$  from the low energy spectrum. This has been called doublet-doublet splitting problem in literature. In the model without HDO contributions, it is clear from the superpotential in Eq. (1) that doublet Higgsino matrix is symmetric:

$$M_H = \begin{pmatrix} \mu_{11} & \mu_{12} \\ \mu_{12} & \mu_{22} \end{pmatrix}. \quad (5)$$

If we now do fine tuning to get one pair of  $H_{u,d}$  at low energies, the  $H_{u,d}$  appear as identical combinations of the doublets in  $\phi_i$ 's. As a result, at the MSSM level, we have proportionality of the  $M_u$  and  $M_d$  leading to vanishing Cabibbo-Kobayashi-Maskawa (CKM) angles. This result holds even if we increase the number of bi-doublets arbitrarily and uses only the fact that bilinear mass matrix  $\mu_{ij}$  is symmetric. This in fact raises the interesting possibility [10] that all mixing angles in the quark and lepton sector may arise purely out of radiative corrections involving the soft breaking terms [11]. An advantage of this version of the model is that there are no new flavor changing effects other than those from the usual supersymmetric sources [12].

On the other hand, one may choose the  $\mu_{ij}$  parameters of this model to be of the order of electroweak scale so that the low-energy model is not exactly the MSSM, but rather the two Higgs pair extension of MSSM. The phenomenology of these models are very similar to the previous case except that there are new contributions to the flavor changing neutral current effects in this model similar to those in the nonsupersymmetric left-right models [13] which puts a lower limit on the masses of the second pair of Higgs doublets to be in the 5–10 TeV range. As a result, they will essentially decouple from the low-energy spectrum.

Our results are independent of which of the above choices for the Higgs sector is made, except that unification discussion applies only to the second version.

### III. GAUGE UNIFICATION

The presence of the doubly charged fields at low energies distinguishes the gauge coupling evolution in this model from the MSSM and one might expect that one will lose the unification property. It, however, turns out that the gauge couplings do unify in this model, albeit at a lower scale as we see below, for the case which has two pairs of Higgs doublets at the weak scale. The couplings evolve according to their respective beta functions. As just mentioned, below the  $v_R$  scale, we assume four Higgs doublet fields instead of

the usual two of MSSM and we assume that one of the doublet pairs has mass of 10 TeV. They lead to a trivial modification of the beta function below  $v_R$ . The beta functions above the  $v_R$  scale are given below for one loop:

$$b_i^{1223} = \begin{pmatrix} 0 \\ -6 \\ -6 \\ -9 \end{pmatrix} + N_F \begin{pmatrix} 2 \\ 2 \\ 2 \\ 2 \end{pmatrix} + n_\Phi \begin{pmatrix} 0 \\ 1 \\ 1 \\ 0 \end{pmatrix} + n_\Delta \begin{pmatrix} 9 \\ 4 \\ 0 \\ 0 \end{pmatrix} + n_{\Delta^c} \begin{pmatrix} 9 \\ 0 \\ 4 \\ 0 \end{pmatrix}, \quad (6)$$

and in the following equation for the two-loop:

$$b_{ij}^{1223} = \begin{pmatrix} 0 & 0 & 0 & 0 \\ 0 & -24 & 0 & 0 \\ 0 & 0 & -24 & 0 \\ 0 & 0 & 0 & -54 \end{pmatrix} + N_F \begin{pmatrix} 7/3 & 3 & 3 & 8/3 \\ 1 & 14 & 0 & 8 \\ 1 & 0 & 14 & 8 \\ 1/3 & 3 & 3 & 68/3 \end{pmatrix} + n_\Phi \begin{pmatrix} 0 & 0 & 0 & 0 \\ 0 & 7 & 3 & 0 \\ 0 & 3 & 7 & 0 \\ 0 & 0 & 0 & 0 \end{pmatrix} + n_\Delta \begin{pmatrix} 54 & 72 & 0 & 0 \\ 24 & 48 & 0 & 0 \\ 0 & 0 & 0 & 0 \\ 0 & 0 & 0 & 0 \end{pmatrix} + n_{\Delta^c} \begin{pmatrix} 54 & 0 & 72 & 0 \\ 0 & 0 & 0 & 0 \\ 24 & 0 & 48 & 0 \\ 0 & 0 & 0 & 0 \end{pmatrix}, \quad (7)$$

where  $i = U(1)_{B-L}, SU(2)_L, SU(2)_R, SU(3)_C$ , respectively in the matrices,  $N_F$  is the number of fermion generations.  $N_F = 3$  always and  $n_\Phi$  is the number of bidoublets which we take to be 2. We also take  $n_\Delta(\Delta + \bar{\Delta})$  and  $n_{\Delta^c}(\Delta^c + \bar{\Delta}^c)$  to be 1. Since the  $\Delta^{\pm\pm}$  leaks down to the weak scale, we need to include its contribution to the running of the gauge couplings in between the weak and the intermediate scale. Since this field  $\Delta$  has only hypercharge quantum number under the SM representation, the hypercharge gauge coupling RGE gets an extra term of  $24/5$  in one loop and in the two loop, the hypercharge squared elements gets an additional factor  $72 \times 16/25$ .

We see from Fig. 1(a) that the gauge couplings unify at a scale  $\sim 10^{11}$  GeV and the intermediate scale is  $\sim 10^8$  GeV. We take  $\alpha_c = 0.118$ ,  $\alpha = 1/128.7$ , and  $\sin^2 \theta_w = 0.2321$  at the weak scale. The low unification scale implies that the proton decay constraint would rule out groups like  $SO(10)$ . However the final unifying group can be  $SU(3) \times SU(3) \times SU(3)$  or any group that conserves baryon number.

In the supergravity motivated models, the gauge unification is necessary in order to have gaugino mass unification. The masses of all the sparticles can then be determined in

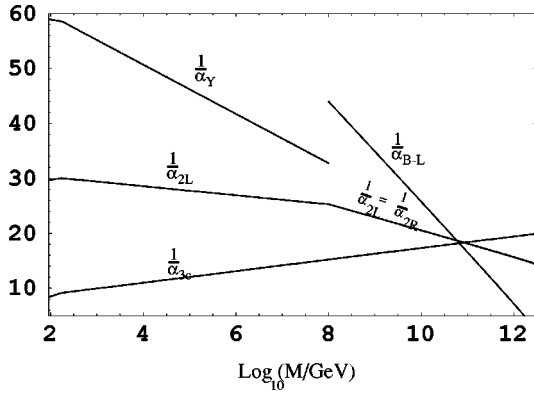


FIG. 1. Gauge coupling unification (two loop) in the supergravity case is shown.

terms of the parameters, e.g., universal scalar mass  $m_0$  at the unification, universal gaugino mass  $m_{1/2}$ , and the trilinear coefficient in the potential  $A$ 's. We choose to assume the universality of  $m_0$  at the unification scale rather than at the Planck scale for two reasons: first is that we do not know the theory above the unification scale and the nature of the evolution of the parameters is obviously dependent on those details. The second reason is that the experimental signature we are interested in involves only the tau lepton and its partner and not the other superparticles of the theory. So even if we assumed universality of scalar masses at the Planck scale which would necessarily imply some splitting between generations due to running between the Planck scale to the unification scale, our final conclusions will be unaffected by this.

We use the quark masses and mixing angle as inputs at the weak scale. The masses we use are:  $m_\tau(m_\tau) = 1.78$  GeV,  $m_t(m_t) = 175$  GeV,  $m_b(m_b) = 4.45$  GeV,  $m_\mu(1 \text{ GeV}) = 0.105$  GeV,  $m_e(1 \text{ GeV}) = 0.51110^{-3}$ ,  $m_u(1 \text{ GeV}) = 0.0044$  GeV,  $m_c(m_c) = 1.27$  GeV,  $m_s(1 \text{ GeV}) = 0.175$  GeV, and  $m_d(1 \text{ GeV}) = 0.008$  GeV. The ratio of the values of the Yukawa coupling at the  $m_t$  scale to the 1 GeV or to the corresponding pole mass scale is given by  $\eta$ . The values of the  $\eta$  we use are  $\eta_u = 2.4, \eta_d = 2.4, \eta_s = 2.4, \eta_c = 2.1, \eta_\tau = 1.0158$  [14]. The Yukawa couplings along with the new coupling between the doubly charged Higgs field and the  $\tau^c$ 's are then evolved to the grand unified theory (GUT) scale in two steps. In the first step we use the MSSM renormalization group equations (RGEs) from the weak scale up to the intermediate scale and then in the second step we use the left right RGEs to evolve up to GUT scale. At the GUT scale, we use the values of these parameters along with  $m_0, m_{1/2}$ , and  $A$  (we will take  $A = 0$ ) as boundary conditions for the RGEs. We evolve the soft breaking masses down to the left right scale using left right RGEs for the soft breaking masses. At the intermediate scale, we introduce the mass for the fermionic and the bosonic component of the  $\Delta$  field, which is generated by the nonrenormalizable operator. We then use the MSSM RGEs to determine the mass spectrum (squarks, sleptons, gauginos, Higgsinos, Higgs) at the weak scale. We determine  $\mu$  at the weak scale from the radiative electroweak breaking conditions. The new parameters in this model are the new mass

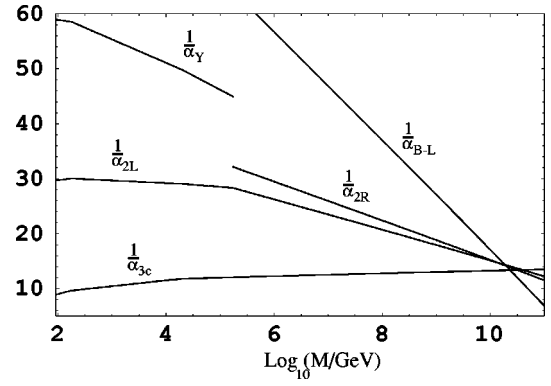


FIG. 2. Gauge coupling unification (two loop) in the GMSB case is shown.

term (which generate both the delta ino and delta boson mass) and the new couplings (coupling of the leptons to the  $\Delta$  field).

If we use GMSB (gauge mediated supersymmetry breaking models) models where SUSY breaking is communicated to the observable sector by gauge mediation, the soft SUSY breaking scalar and the gaugino masses are generated at a scale  $\sim 10^5$  GeV by gauge interactions (see Fig. 2). In this type of models gauge unification is not necessary in order to have unified gaugino mass, since they are generated in one loop. In our calculation for the GMSB cases, we do not consider any gauge unification. However in Fig. 1(b) we show one example where we have the gauge unification with a messenger sector composed of: one copy of  $D_R + \bar{D}_R, U_R + \bar{U}_R$ , and  $L_L + \bar{L}_L$ . The couplings unify at  $10^{10.5}$  GeV, the intermediate scale is at  $\sim 10^{5.2}$  GeV, and the  $\alpha_R/\alpha_{B-L}$  is 1/2 at the intermediate scale.

In the GMSB case we evolve the Yukawa couplings up to the messenger scale, which is lower than the intermediate scale. We then evolve the soft masses down to the weak scale using the MSSM RGEs and determine the particle spectrum.

#### IV. GRAVITY MEDIATED SCENARIO

In the standard gravity mediated scenarios, one starts with a universal mass-square for all scalar components of the chiral superfields at the Planck scale and they are then extrapolated to the weak scale to determine their masses [15]. For those fields with large Yukawa couplings such as the Higgs doublet  $H_u$ , top squark, the weak scale value is significantly lower than the Planck scale one. (In fact, for the  $H_u$  turning negative gives rise to the celebrated phenomenon of radiative electroweak symmetry breaking.) For other squarks, the gaugino mass contribution has the effect of increasing their value over the Planck scale value. On the other hand for the sleptons, the change between the weak scale and Planck scale value is not very significant since they neither have large Yukawa couplings nor do they have strong interactions.

Turning now to the SUSYLR model, as mentioned before, we will assume universality at the unification and in contrast with the MSSM, the effective theory below the right handed

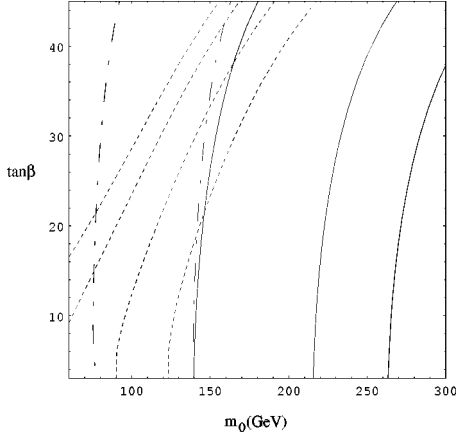


FIG. 3. The mass contours for  $M_{\tilde{\Delta}^{\pm\pm}} = 90$  GeV at the intermediate scale and  $f_3 = 0.5$  are shown. The  $\tilde{\tau}_1$  mass contours (dashed line) from left to right depict 45, 60, 80, and 100 GeV masses, the  $\Delta^{\pm\pm}$  mass contours (solid lines) from left to right depict 88, 70, and 50 GeV masses, the  $\tilde{e}_R$  ( $\tilde{e}_R$  and  $\tilde{\mu}_R$  masses are the same) mass contours (dot-dashed line) from left to right depict 100 and 140 GeV masses.

scale, contains the following new coupling in the superpotential:

$$W_{extra} = f_i \Delta^{\pm\pm} l_i^c l_i^c \quad (8)$$

which will have a major impact on our spectrum at the weak scale.

In writing the above coupling, we have used the fact that experimental limits on lepton flavor changing processes such as  $\mu \rightarrow 3e$  and  $\tau \rightarrow 3e$  imply that  $f_{ij}$  with  $i \neq j$  are very small compared to the diagonal couplings  $f_i$  and have, therefore, taken the liberty to simply drop the off-diagonal couplings. In what follows, we will denote  $\Delta^c \equiv \Delta$ . This interaction gives rise to the process  $\mu^+ e^- \rightarrow \mu^- e^+$  with a strength

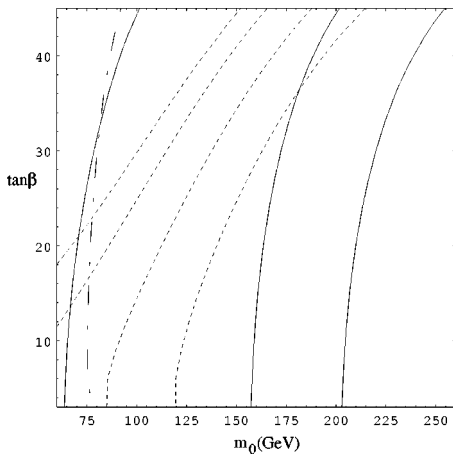


FIG. 4. The mass contours for  $M_{\tilde{\Delta}^{\pm\pm}} = 70$  GeV at the intermediate scale and  $f_3 = 0.5$  are shown. The  $\tilde{\tau}_1$  mass contours (dashed line) from left to right depict 45, 60, 80, and 100 GeV masses, the  $\Delta^{\pm\pm}$  mass contours (solid lines) from left to right depict 80, 65, and 50 GeV masses, the  $\tilde{e}_R$  mass contour (dot-dashed line) depicts 100 GeV mass.

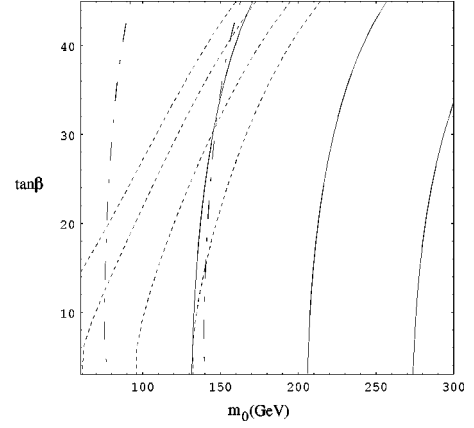


FIG. 5. The mass contours for  $M_{\tilde{\Delta}^{\pm\pm}} = 110$  GeV at the intermediate scale and  $f_3 = 0.5$  are shown. The  $\tilde{\tau}_1$  mass contours (dashed line) from left to right depict 45, 60, 80, and 100 GeV masses, the  $\Delta^{\pm\pm}$  mass contours (solid lines) from left to right depict 108, 95, and 70 GeV masses, the  $\tilde{e}_R$  mass contours (dot-dashed line) from left to right depict 100 and 140 GeV masses.

$G_{M-\bar{M}} \approx f_1 f_2 / 4 \sqrt{2} M_\Delta^2$ . Recent PSI experiment [8] has yielded an upper limit on  $G_{M-\bar{M}} \leq 3 \times G_F \times 10^{-3}$ . For  $M_\Delta = 100$  GeV, this implies that  $f_1 f_2 \leq 1.2 \times 10^{-3}$ . Thus we expect each of the couplings to be less than 0.1 barring pathological situations where only one of the couplings bears the brunt of the constraint. On the other hand, there is no such constraint on  $f_3$  from experiments. So we will choose it to be of order 0.5. Thus, there are only two new parameters in the theory, the new mass term and the coupling  $f_3$ .

The first implication of the relatively large  $f_3$  is on the weak scale value for the mass of the  $\Delta$ -boson. As shown in [6], at the  $\nu_R$  scale, both the  $\Delta$  and its fermionic partner  $\tilde{\Delta}$  ( $\Delta$ -ino) have nearly the same mass. The bosonic component, however, runs faster than the fermionic one. As a result, at low energies we can expect that  $M_\Delta < M_{\tilde{\Delta}}$ . This has important implications for phenomenology.

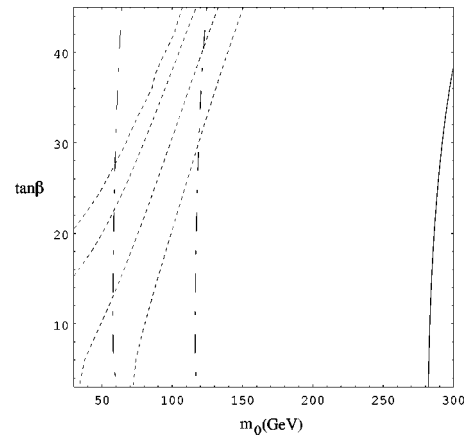


FIG. 6. The mass contours for  $M_{\tilde{\Delta}^{\pm\pm}} = 90$  GeV at the intermediate scale and  $f_3 = 0.25$  are shown. The  $\tilde{\tau}_1$  mass contours (dashed line) from left to right depict 45, 60, 80, and 100 GeV masses, the  $\Delta^{\pm\pm}$  mass contour (solid lines) depicts 88 GeV, the  $\tilde{e}_R$  mass contours (dot dashed line) from left to right depict 100 and 140 GeV masses.

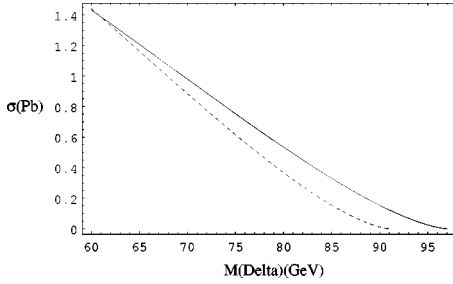


FIG. 7. The  $\Delta^{\pm\pm}$  pair production GeV at the cross section at LEP II. The solid and the dotted line correspond to the cross sections at the center of mass energies to be 194 GeV and 182 GeV.

A second consequence of the possible large  $f_3$  is that the  $\tilde{\tau}^c$  mass is drawn down to smaller values at lower scales. In order to calculate the mass spectrum, we use the algorithm described in the previous section. We use the RGE's shown in the Appendix and in the Refs. [16–18]. We determine the parameter  $\mu$  from the condition that electroweak symmetry is broken radiatively. We choose the sign of  $\mu$  to be negative, since the other choice will give large  $b \rightarrow s \gamma$  rate. The lighter stau mass will be much smaller than the other sleptons (even when  $\tan\beta$  is small) due to the presence of the new coupling  $f_3$ . In Fig. 3 we show the mass contours of the lighter stau (dotted line), the  $\Delta^{\pm\pm}$  (solid line), and the lighter selectron (dot-dashed line) in the  $m_0$  and  $\tan\beta$  plane for  $m_{1/2} = 180$  GeV. We choose  $\tilde{\Delta}^{\pm\pm}$  mass  $\sim 100$  GeV at the weak scale (90 GeV at the intermediate scale). As  $m_0$  increases the  $\Delta^{\pm\pm}$  mass decreases due to the subtractive effect in the RGE originating from the larger soft SUSY breaking scalar mass. We can see from the figure that the bound on  $\Delta^{\pm\pm}$  mass rules out the upper range of  $m_0$ . The lower bound on lighter stau ( $\tilde{\tau}_1$ ) mass on the other hand rules out lower range of  $m_0$ .

The latest bound on lighter stau mass is about 57 GeV [19]. In this scenario  $\tilde{\Delta}^{\pm\pm}$  mass is too high to be pair produced at LEP II. We also observe (due to the smallness of  $f_{1,2}$  compared to  $f_3$ ) that the lighter selectron mass is much higher than the  $\tilde{\tau}_1$  mass even when the  $\tan\beta$  is small for the same  $m_0$  and  $m_{1/2}$  values. This will differentiate between the final states of chargino pair production in MSSM and in this model. In Fig. 4 we show the same mass contours for  $\tilde{\Delta}^{\pm\pm} \sim 80$  GeV at the weak scale (70 GeV at the intermediate scale). Lower  $\Delta^{\pm\pm}$  mass indicates lesser effect on the  $\tilde{\tau}_1$  mass from the new interactions and, consequently, more parameter space for lower  $m_0$ , however, low  $\Delta$  mass rule out more parameter space from the higher  $m_0$  range. In this scenario the  $\tilde{\Delta}^{\pm\pm}$ 's can be pair produced at LEP II. In Fig. 5 we exhibit a scenario where  $\tilde{\Delta}$  mass is  $\sim 120$  GeV at the weak scale (110 GeV at the intermediate scale). The lightest neutralino ( $\chi_1^0$ ) in all these scenarios are  $\sim 49$ –57 GeV and the lightest chargino mass is around 80–90 GeV. If we vary the  $m_{1/2}$ , e.g.,  $m_{1/2} = 150$  GeV, the  $\chi_1^0$  becomes 33–43 GeV and the lightest chargino becomes 57–67 GeV. The scalar masses also get reduced by 10–20 GeV. In Fig. 6 we show a scenario where the third generation coupling is smaller  $f_3$

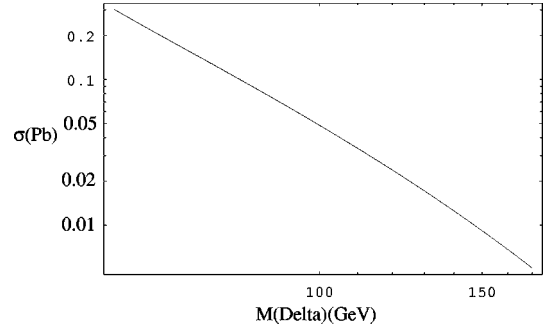


FIG. 8. The  $\Delta^{\pm\pm}$  pair production cross section at Tevatron (center of mass energy is 2 TeV).

$\sim 0.25$ . As one can expect, the effect of the new couplings in the stau mass is reduced. For low  $\tan\beta$ , as in the conventional SUGRA mode, the  $\tilde{\tau}_1$  and the lighter selectron mass ( $\tilde{e}_R$ ) become very close. The  $\Delta$  boson mass lower than 88 GeV appears for  $m_0 > 270$  GeV, whereas in Fig. 3 the same mass contour appears at  $m_0 > 140$  GeV. (In both the cases the  $m_{1/2}$  at the GUT scale and  $M_{\tilde{\Delta}}$  at the intermediate scale are same.) From the analysis of the parameter space, we surmise that most of the allowed parameter space for large  $f_3$  can be searched in the present colliders or in the colliders to be upgraded in the near future.

The  $\Delta$  will decay into a pair of  $\tau$ 's (since the coupling to the other leptons are suppressed). The  $\tau$ 's have high  $p_T$ . We have 4  $\tau$ 's in the final state. The like charged  $\tau$ 's originate from the same vertex.

The SM background for this process can come from the pair production of  $Z^0$  and the subsequent decay of each  $Z^0$  to a  $\tau^+ \tau^-$  pair (in all these cases oppositely charged  $\tau$ 's come from the same vertex). This event will have no missing energy, but the rate is small due to the small branching ratio for  $Z^0 \rightarrow \tau^+ \tau^-$  ( $\sigma \cdot B^2 \sim 10^{-3}$  pb). The  $4\tau$  background can also come from the production of  $Z\gamma^*$ ,  $\gamma^*$  converting into  $\tau^+ \tau^-$  and the  $Z$  decaying into  $\tau^+ \tau^-$  pair. Another source can be the production of two virtual photons along with  $e^+ e^-$  and each photon converting into  $\tau^+ \tau^-$ . However, in both the above processes, the cross section is  $\sim 10^{-3}$  pb. Thus, the SM background is negligible small for the  $4\tau$  signal.

The  $\tilde{\Delta}$  will primarily decay into  $\tilde{\tau}_1$  and  $\tau$  (almost 100%). The  $\tilde{\tau}_1$  will then decay into  $\tau$  and  $\chi_1^0$  (missing energy) (100%). The final state has 4  $\tau$ 's plus missing energy. Two of the  $\tau$ 's have high  $p_T$  and these originate from the decay of lighter stau. This kind of 4  $\tau$  plus missing energy signal also originate from the  $\chi_1^0$  pair production in the GMSB scenarios where lighter stau is the NLSP. But there is a subtle difference in the final state which we will discuss in the next section.

The chargino pair production can also give rise to  $2\tau$  plus missing energy states. Since the staus are much lighter than the other sleptons, the chargino will primarily decay into  $\tilde{\tau}_1$  and  $\nu_\tau$  in the leptonic decay channel. On the other hand, the chargino decays into  $e$ 's and  $\mu$ 's as well as  $\tau$ 's in the MSSM. The charginos can be pair produced at LEP II and Tevatron. The production of chargino and the second lightest

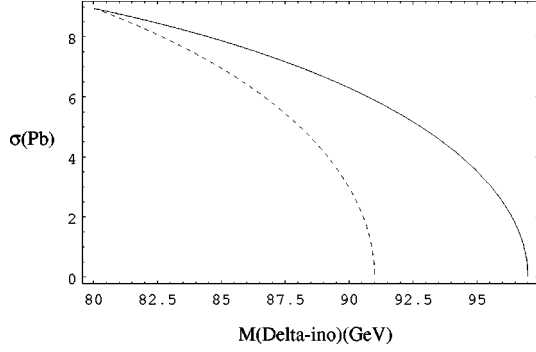


FIG. 9. The  $\tilde{\Delta}^{\pm\pm}$  pair production cross section at LEP II. The solid line and the dotted line correspond to the cross section at the center of mass energies to be 194 GeV and 182 GeV, respectively.

neutralino (this cross section is larger than the chargino pair production) at the Tevatron will also give rise to lots of high  $p_T$  taus in the final state. The second lightest neutralino ( $\chi_2^0$ ) primarily decays into  $\tau$  and  $\tilde{\tau}_1$  and  $\tilde{\tau}_1$  then decays into a tau and the lightest neutralino. Altogether, there can be  $3\tau$ 's along with missing energy. Since  $\chi_2^0$  mass is much larger than the  $\tilde{\tau}_1$  mass, all the three  $\tau$ 's will have high  $p_T$ .

The  $\Delta$  bosons and the  $\Delta$ -inos can be pair produced at the LEP II and at the Tevatron as well. The productions of  $\Delta$ 's (fermion and boson) at LEP II and  $\Delta$  scalar at Tevatron have been considered in the Ref. [20].

The  $\tilde{\Delta}$  pair production cross section in a  $f\bar{f}$  interactions is

$$\sigma_{\tilde{\Delta}} = \frac{4\alpha^2\pi\beta}{3s} \left( 1 + \frac{2M_{\tilde{\Delta}^2}}{s} \right) \left( Q_f^2 Q_D^2 + \frac{s^2(g_{fA}^2 + g_{fv}^2)g_{Dv}^2}{(s - M_Z^2)^2 + \Gamma_Z^2 M_Z^2} \right. \\ \left. + \frac{2sQ_f Q_D (s - M_Z^2) g_{fv} g_{Dv}}{(s - M_Z^2)^2 + \Gamma_Z^2 M_Z^2} \right), \quad (9)$$

where  $g_{fv} = I_{3f} - 2Q_f \sin^2 \theta_w / 2 \sin \theta_w \cos \theta_w$ ,  $g_{fA} = I_{3f} / 2 \sin \theta_w \cos \theta_w$ , and  $D$  stands for the  $\tilde{\Delta}$ .  $Q_f$  and  $I_{3f}$  are electric charge and the isospin of the fermions and  $Q_D$  is the electric charge of the  $\tilde{\Delta}$ .

The  $\Delta$  pair production in a  $f\bar{f}$  interactions is

$$\sigma_{\Delta} = \frac{\alpha^2\pi\beta^3}{3s} \left( Q_f^2 Q_D^2 + \frac{2s^2(g_{fA}^2 + g_{fv}^2)g_{Dv}^2}{(s - M_Z^2)^2 + \Gamma_Z^2 M_Z^2} \right. \\ \left. + \frac{2sQ_f Q_D (s - M_Z^2) g_{fv} g_{Dv}}{(s - M_Z^2)^2 + \Gamma_Z^2 M_Z^2} \right). \quad (10)$$

We show the production cross sections of the  $\Delta$  bosons at the LEP II and at the Tevatron in Figs. 7 and 8. The  $\Delta$ -ino is pair produced at the LEP II and at the Tevatron via  $Z$ ,  $\gamma$  exchange. Usually there is also a selectron mediated t-channel contribution in the case of  $\Delta$ -ino production at the  $e^+e^-$  collider. However the contribution from this diagram in this model is negligible since the  $\Delta$  coupling to the first generation leptons is very small. The production cross sections are larger than the scalar counterparts for the same mass. In Fig. 9 we show the production of  $\tilde{\Delta}$  at LEP II for

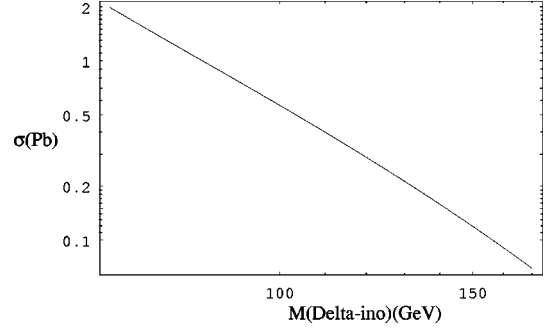


FIG. 10. The  $\tilde{\Delta}^{\pm\pm}$  pair production cross section at Tevatron (center of mass energy is 2 TeV).

$\sqrt{s} = 182$  GeV and 194 GeV. We can see that the  $\Delta$ -ino mass of 95 GeV gives rise to a cross section of 3 pb at LEP II. Thus, if the  $\Delta$ -inos are produced at LEP II, the cross section will be quite large.

In Fig. 10 we show the production cross section at the Tevatron for  $\sqrt{s} = 2$  TeV. The production cross section is about 0.7 pb at  $\sqrt{s} = 2$  TeV for  $\Delta$ -ino mass of 95 GeV and the cross section is about 0.6 pb at  $\sqrt{s} = 1.8$  TeV for the same  $\Delta$ -ino mass. Hence, with  $110 \text{ pb}^{-1}$  of already accumulated luminosity, the number of events are  $\sim 66$ . Since the final state are pure  $\tau$  leptons, detection is difficult. But we will have some events left even after taking the  $\tau$  detection efficiency to be small. We urge the experimentalists to look for the  $\tau$  signals in the data which has been already accumulated and also in the data that will be generated in the future runs.

## V. GAUGE MEDIATED SUSY BREAKING SCENARIO

In the previous section we assumed that the scale at which supersymmetry is broken is higher than the  $W_R$  scale. However this need not be the case and, in particular, there has recently been a lot of interest in theories where gauge interactions are the mediators of supersymmetry breaking at a relatively low scale [9]. Let us discuss the implications of this scenario for our model. The soft SUSY breaking terms are now generated explicitly only at the scale at which the messenger fields are integrated out, and are not explicitly present at the  $W_R$  scale. Since they are generated by loop graphs involving the gauge bosons of the residual symmetries, their form will be such as to respect only the surviving gauge symmetries. We will show that this difference has consequences for phenomenology. Let us assume for simplicity that the messenger sector consists of a vectorlike isosinglet pair of fields (charge  $-1/3$ )  $Q \oplus \bar{Q}$  and a vectorlike weak isodoublet pair  $L \oplus \bar{L}$ .

As shown in [6], in this case, the scalar  $\Delta$  mass has two contributions at the SUSY breaking scale of 100 TeV or so: one coming from the two loop gauge contributions in the usual manner (for a review see [15]) and another coming from the higher dimensional terms. On the other hand, the  $\tilde{\Delta}$  mass gets contribution only from the latter kind of terms. We, therefore, expect that in the gauge mediated scenario,

the  $\tilde{\Delta}$  will be the lighter of the two particles.

The soft SUSY breaking gaugino and the scalar masses at the messenger scale  $M$  are given by [15]

$$\tilde{M}_i(M) = n g \left( \frac{\Lambda}{M} \right) \frac{\alpha_i(M)}{4\pi} \Lambda$$

and

$$\tilde{m}^2(M) = 2n f \left( \frac{\Lambda}{M} \right) \sum_{i=1}^3 k_i C_i \left( \frac{\alpha_i(M)}{4\pi} \right)^2 \Lambda^2,$$

where  $\alpha_i$  ( $i=1-3$ ) are the three SM gauge couplings and  $k_i=1,1,3/5$  for SU(3), SU(2), and U(1), respectively. The  $C_i$  are zero for gauge singlets, and  $4/3$ ,  $3/4$ , and  $(Y/2)^2$  for the fundamental representations of SU(3) and SU(2) and U(1) $_Y$ , respectively (with  $Y$  defined by  $Q=I_3+Y/2$ ). Here  $n$  corresponds to  $n((Q,L)+(\bar{Q},\bar{L}))$ .  $g(x)$  and  $f(x)$  are messenger scale threshold functions with  $x=\Lambda/M$ .

We calculate the SUSY mass spectrum using the appropriate RGE equations [16] with the boundary conditions given by the equations above and we vary five free parameters  $\Lambda$ ,  $M/\Lambda$ ,  $\tan\beta$ ,  $n$ , and the sign of  $\mu$  ( $\mu$  is the coefficient of the bilinear Higgs term in the superpotential). We first run the Yukawa couplings (along with the three new couplings  $f_{1,2,3}$ ) and gauge couplings from the weak scale up to the GMSB scale. At the GMSB scale we use the boundary conditions and then use the necessary RGEs for the soft SUSY breaking masses in order run down to the weak scale.

The CLEO constraint on the  $b \rightarrow s \gamma$  rate restricts  $\mu < 0$  [21]. In the absence of late inflation, cosmological constraints put an upper bound on the gravitino mass of about  $10^4$  eV [22], which restricts  $M/\Lambda = 1.1-10^4$ . In the figures we show the results for  $n=1$ , but we discuss the other values of  $n$  also. For reasons discussed before, we assume that  $f_{1,2}$  are small ( $\sim 0.05$ ), but  $f_3$  is larger. We show our result for  $f_3 \sim 0.5$  and  $f_3 \sim 0.25$ . We also vary  $M_{\tilde{\Delta}}$  between 70–120 GeV at the GMSB scale.

The gravitino is always the lightest supersymmetric particle (LSP). In the usual GMSB case the  $\chi_1^0$  and the  $\tilde{\tau}_1$  fight for the next LSP (NLSP) spot. In this model the  $\tilde{\Delta}^{\pm\pm}$  also joins the race to become NLSP. The third generation lighter stau mass gets affected due to the presence of the additional large coupling  $f_3$ . Thus, the  $\tilde{\tau}_1$  is much smaller compared to the conventional GMSB case for the same parameter space. Consequently, the lighter stau will be the NLSP for a wider region of parameter space compared to the lighter neutralino.

In Fig. 11(a) we have shown the mass contours of  $\tilde{\tau}_1$  (solid line),  $\tilde{e}_R$  (dotted line),  $\chi_1^0$  (dash-dotted line), and the chargino masses (dashed line) for  $M=1.1\Lambda$ ,  $n=1$ , and  $M_{\tilde{\Delta}}=90$  GeV at the GMSB scale (94 GeV at the weak scale). We also show the contour along which the lighter stau mass and the neutralino mass are same (thick solid line). The region above the contour has lighter stau as the NLSP. We see that only a small region for  $\tan\beta$  3–15 and  $\Lambda$  40–60 TeV has  $\chi_1^0$  as NLSP. When  $\chi_1^0$  is the NLSP, it decays into a photon and a gravitino. If  $\chi_1^0$  is pair produced at LEP II, the

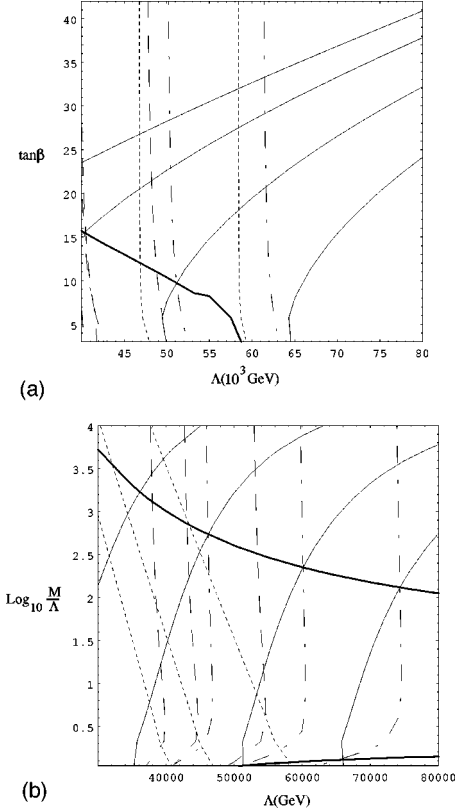


FIG. 11. (a) The mass contours for  $M_{\tilde{\Delta}^{\pm\pm}}=90$  GeV at the GMSB scale and  $f_3=0.5$  are shown. The  $\tilde{\tau}_1$  mass contours (solid line) from left to right depict 45, 60, 80, and 100 GeV masses, the  $\tilde{e}_R$  mass contours (dotted lines) depict 80 (along the left axis), 95 and 115 GeV masses, the  $\chi_1^0$  (dot-dashed) mass contours depict 60, 80, and 100, GeV masses, the lightest chargino ( $\chi^\pm$ ) mass contours (dashed) depict 94, 100, and 130 GeV masses. (b) The mass contours for  $M_{\tilde{\Delta}^{\pm\pm}}=90$  GeV at the GMSB scale and  $f_3=0.5$  are shown. The  $\tilde{\tau}_1$  mass contours (solid line) from left to right depict 45, 60, 80, and 100 GeV masses, the  $\tilde{e}_R$  mass contours (dotted lines) depict 80, 95, and 115 GeV masses, the  $\chi_1^0$  (dot-dashed) mass contours depict 60, 80, and 100 GeV masses, the lightest chargino mass contours (dashed) depict 88, 100, and 130 GeV masses. The thick solid lines in both the figures depict the contour along which the lighter stau mass equals to the lightest neutralino mass.

final state has  $\gamma\gamma$  plus  $\tilde{E}_T$ . The photons are hard and easy to detect. Already we have bound on the  $\chi_1^0$  mass of around 80 GeV at LEP II [23] provided the selectrons are not too heavy. We can see that if we use  $\chi_1^0$  mass bound as 80 GeV, the region left out in Fig. 11(a) where  $\chi_1^0$  is the NLSP is very small. The region where  $\tilde{\tau}_1$  is the NLSP, which is the dominant region, stau decays into a high  $p_T$   $\tau$  and a gravitino (missing energy). So far there is not much bound in these regions, other than the  $\tilde{\tau}_1$  has to be larger than 57 GeV. In the figures we have shown the stau mass contours of 45, 60, 80, and 100 GeV. The  $\tilde{\tau}_1$  mass contours have large dependence on the  $\tan\beta$ , the  $\tilde{\tau}_1$  decreases with the increase in  $\tan\beta$ . The  $\tilde{e}_R$ , chargino and the  $\chi_1^0$  mass contours do not have much  $\tan\beta$  dependence.

In Fig. 11(b) we show the same mass contours in the



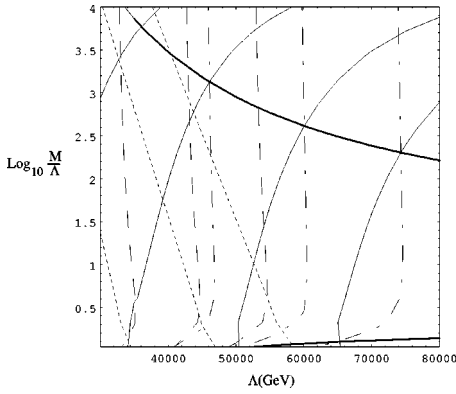


FIG. 12. The mass contours for  $M_{\tilde{\Delta}^{\pm\pm}} = 70$  GeV at the GMSB scale and  $f_3 = 0.5$  are shown. The  $\tilde{\tau}_1$  mass contours (solid line) from left to right depict 45, 60, 80, and 100 GeV masses, the  $\tilde{e}_R$  mass contours (dotted lines) depict 75, 95, and 115 GeV masses, the  $\chi_1^0$  (dot-dashed) mass contours depict 60, 80, and 100 GeV masses, the lightest chargino mass contours (dashed) depict 70, 100, and 130 GeV masses. The thick solid lines depict the contour along which the lighter stau mass equals to the lightest neutralino mass.

plane of  $\Lambda$  and  $M/\Lambda$  for  $\tan\beta = 10$ . The contours along which  $\tilde{\tau}_1$  mass is equal to the  $\chi_1^0$  mass form an envelope. Within the envelope  $\chi_1^0$  is NLSP. The  $\tilde{e}_R$  masses increase as the  $M/\Lambda$  ratio increase. The couplings  $f_{1,2}$  are small to affect the  $\tilde{e}_R$  or the  $\tilde{\mu}_R$  masses (selectron and smuon masses are almost the same). The lighter stau mass, however, decreases with the increase in the ratio of  $M/\Lambda$  (subtractive effect from the soft scalar masses due to the presence of the new coupling overcome effects coming from the gaugino masses in the RGE). In the conventional GMSB model, the stau mass increases with the increase in the  $M/\Lambda$  ratio. With the improvement of the  $\tilde{\tau}_1$  mass bound much more parameter space will be ruled out in the higher  $M/\Lambda$  ratio. The  $\chi_1^0$  and the chargino masses initially decrease with the increase in the ratio of  $M/\Lambda$  due to the threshold corrections. The 80 GeV  $\chi_1^0$  bound rules out much of the parameter space in the envelope where  $\chi_1^0$  is the NLSP. The  $M_{\tilde{\Delta}^{\pm\pm}}$  varies between 94–108 GeV at the weak scale. Unlike the supergravity (SUGRA) scenario, the  $\Delta^{\pm\pm}$  mass is much larger than the fermionic part at the weak scale and its mass, in the full range shown in the figure, varies from 170–570 GeV (due to the large soft SUSY breaking contribution at the GMSB scale). Thus, the allowed parameter space in GMSB scenarios are much more than the SUGRA scenarios.

In Figs. 12 and 13, we have shown the mass contours in the  $\Lambda$ - $M/\Lambda$  plane for  $M_{\tilde{\Delta}^{\pm\pm}} = 70$  and 110 GeV at the GMSB scale. The  $\tan\beta$  is chosen to be 10. When  $M_{\tilde{\Delta}^{\pm\pm}} = 70$  GeV, the envelope is larger, since  $\tilde{\tau}_1$  mass has less subtractive contribution from the delta mass. On the other hand, when  $M_{\tilde{\Delta}^{\pm\pm}} = 110$  GeV, the envelope shrinks. The envelope can also increase in the size if we have smaller coupling  $f_3$ . We show the effect of a smaller  $f_3$  in Fig. 14. This figure looks more like the conventional GMSB model. We see that there is no parameter space where  $\tilde{\tau}_1$  is NLSP. But if we increase  $\tan\beta$  we will hit the region where  $\tilde{\tau}_1$  is

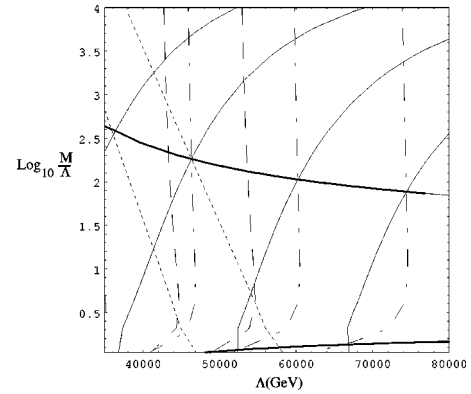


FIG. 13. The mass contours for  $M_{\tilde{\Delta}^{\pm\pm}} = 110$  GeV at the GMSB scale and  $f_3 = 0.5$  are shown. The  $\tilde{\tau}_1$  mass contours (solid line) from left to right depict 45, 60, 80, and 100 GeV masses, the  $\tilde{e}_R$  mass contours (dotted lines) depict 95 and 115 GeV masses, the  $\chi_1^0$  (dot-dashed) mass contours depict 60, 80, and 100 GeV masses, the lightest chargino mass contours (dashed) depict 100 and 130 GeV masses. The thick solid lines depict the contour along which the lighter stau mass equals to the lightest neutralino mass.

the NLSP. The  $\tilde{\tau}_1$  mass in this case, as expected, increases with the increases in the ratio of  $M/\Lambda$ . So far in all these figures we have used  $n = 1$ . The effect of larger values of  $n$  can easily be surmised from the mass formula. As  $n$  increases gaugino masses increase proportionally, on the other hand the scalar masses increase as  $\sqrt{n}$ . Hence, stau mass is the NLSP for a even wider region of parameter space. The lighter selectron's mass becomes closer to the lighter stau mass and lower than the neutralino mass.

Let us now discuss the signals. At LEP II, the main production processes are the  $\chi_1^0$  pair, the  $\tilde{\Delta}^{\pm\pm}$  pair, the  $\tilde{e}_R$  pair and the  $\tilde{\tau}_1$  pair.

In the case of  $\tilde{\Delta}^{\pm\pm}$  pair production, each  $\tilde{\Delta}^{\pm\pm}$  will decay primarily into a  $\tilde{\tau}_1$  and a tau (both having same sign of charge). The other decay modes involving, e.g., a electron

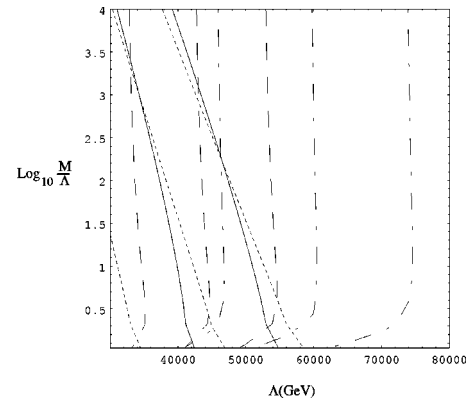


FIG. 14. The mass contours for  $M_{\tilde{\Delta}^{\pm\pm}} = 90$  GeV at the GMSB scale and  $f_3 = 0.25$  are shown. The  $\tilde{\tau}_1$  mass contours (solid line) from left to right are 80 and 100 GeV, the  $\tilde{e}_R$  mass contours (dotted lines) are 75, 95, and 115 GeV, the  $\chi_1^0$  (dot-dashed) mass contours are 60, 80, and 100 GeV, the lightest chargino mass contours (dashed) are 70, 100, and 130 GeV.

and a  $\tilde{e}_R$  and a muon and a smuon are suppressed primarily because of small  $f_{1,2}$  couplings. In the parameter space when stau is the NLSP,  $\tilde{\Delta}^{\pm\pm}$  decays into a  $\tilde{\tau}_1$  and a  $\tau$  and  $\tilde{\tau}_1 \rightarrow \tau\tilde{G}$ . Thus, the final state has  $4\tau$  plus missing energy and out of the  $4\tau$ 's, two have high  $p_T$  (higher  $p_T$  than the SUGRA case). These two high  $p_T$   $\tau$ 's have opposite sign electric charges.

The  $\chi_1^0$  pair production also gives rise to  $4\tau$ 's plus missing energy (since each  $\chi_1^0 \rightarrow \tilde{\tau}_1\tau$ ), with two of these  $\tau$ 's having high  $p_T$  [24]. However there is an essential difference between the signal in this case and in the previous case. Since the neutralino is a majorana particle, the two high  $p_T$   $\tau$ 's can have same or opposite sign (with equal probability) for the electric charges and thus providing a way to discriminate between the two cases.

In the case of  $\tilde{e}_R$  pair productions, each selectron will either decay into an electron and a  $\chi_1^0$  or a  $\tilde{\Delta}^{\pm\pm}$  and a positron (if the selectron mass is higher than the  $\chi_1^0$  mass and the  $\tilde{\Delta}^{\pm\pm}$  mass). Both  $\chi_1^0$  and  $\tilde{\Delta}^{\pm\pm}$  decay to  $2\tau$  plus missing energy. The final states in either case will have  $2e4\tau$  plus missing energy with two of the  $\tau$ 's having high  $p_T$ . Their relative sign will determine the decay channel of the selectron. If, however, the  $\tilde{e}_R$  mass is lower than both the  $\chi_1^0$  mass (large  $n$  case) and the  $\tilde{\Delta}^{\pm\pm}$  mass, the selectron can decay into an electron and a gravitino or via offshell production of the  $\chi_1^0$  or  $\tilde{\Delta}^{\pm\pm}$ . The  $\chi_1^0$  and  $\tilde{\Delta}^{\pm\pm}$  then convert into  $2\tau$  plus missing energy. In the former case the final state of the selectron pair production has  $2e$  plus missing energy and in the later case the signal is  $2e4\tau$  plus missing energy. Depending on the parameter space, these offshell decay modes can be comparable or greater than the onshell decay mode [25]. In the case of smuons, the electrons in the final states will be replaced by the muons.

When  $\chi_1^0$  is the NLSP, the  $\tilde{\Delta}^{\pm\pm}$  will decay into a  $\tilde{\tau}_1$  and a  $\tau$  (100%). The  $\tilde{\tau}_1$  will decay into a  $\chi_1^0$  and a  $\tau$ . The  $\chi_1^0$  then decays into a photon and a gravitino. All the branching ratios are 100%. The final state from the  $\tilde{\Delta}^{\pm\pm}$  pair production will have  $2\gamma4\tau$  plus missing energy, which is a spectacular signal and very hard to miss. This signal will appear along with the electrons or the muons in the case of selectron or smuon production, where the selectron decays as described above, i.e.,  $\tilde{e}_R \rightarrow e\tilde{\Delta}^{\pm\pm}$ .

In the conventional GMSB models when  $\chi_1^0$  is the NLSP case, one gets at most 2 leptons along with  $2\gamma$  (through the slepton productions whose cross section is much smaller than the delta-ino production cross section) at the LEP II and at the Fermilab Tevatron or 3 leptons plus 2 photons (chargino-second lightest neutralino production) at the Tevatron. Thus, the signal  $2\gamma4\tau$  plus missing energy will clearly distinguish this model from the ordinary GMSB models in the parameter space where  $\chi_1^0$  is the NLSP. It may also happen that the  $\tilde{\Delta}^{\pm\pm}$  mass is smaller than the  $\tilde{\tau}_1$  or the  $\chi_1^0$  mass. In that case the  $\tilde{\Delta}^{\pm\pm}$  will decay into a  $\tau$  and a virtual  $\tilde{\tau}_1$  which will convert into a  $\tau$  plus gravitino or if the  $\chi_1^0$  mass is lower than the  $\tilde{\tau}_1$  mass, then the  $\tilde{\tau}_1$  will decay into a  $\tau$  and a

$\chi_1^0$ . The  $\chi_1^0$  will then convert into a photon and the gravitino. Thus the final states are same as discussed in the cases when  $\chi_1^0$  is the NLSP or  $\tilde{\tau}_1$  is the NLSP.

## VI. CONCLUSION

To summarize, we have studied the phenomenological implications and the collider signatures of the remnant doubly charged Higgs boson  $\Delta^{\pm\pm}$  and its fermionic partner the Deltaino  $\tilde{\Delta}^{\pm\pm}$ . We find that existing limits on lepton flavor violation and muonium-anti-muonium transition can be used to conclude that the dominant coupling of these particles are diagonal and mostly to the third generation of leptons. The new couplings of course are forbidden from coupling to the quarks by electric charge conservation. The effect of the dominant third generation lepton coupling has the consequence that the  $\tilde{\tau}_1$  mass is much smaller than the other slepton masses. This gives rise to multiple  $\tau$  enriched signal at LEP II and Tevatron. The fermionic as well as the bosonic partner of the doubly charged Higgs bosons can be produced at the present colliders and the signals contain  $4\tau$  (plus  $2\gamma$  in some scenarios of the GMSB version of the models) with and without missing energy. This signal is found to be detectable for reasonable range of mass values of the particles and could be used to test the supersymmetric left-right models of the type discussed here or to restrict the allowed parameter range of the model. Most of the allowed parameter space can be searched in the existing colliders. We, therefore, urge the experimentalists to analyze the tau events in the existing as well as in the future data.

## ACKNOWLEDGMENTS

The work of R. N. M. has been supported by the National Science Foundation Grant No. PHY-9421385 and that of B. D. by Grant No. DE-FG06-854ER 40224. We thank G. Altarelli, J. Gunion, and G. Snow for encouragement and comments.

## APPENDIX

The standard MSSM RGEs for the Yukawa couplings and the soft SUSY breaking terms will be modified due to the presence of the new couplings and the fields. There will be new RGEs for the additional fields and the couplings. The new interaction involves the third generation right-handed leptons and the new field  $\Delta^{\pm\pm}$ . We will keep only the  $f_3$  coupling in the RGE's (in our numerical calculation we use all of them). The new RGEs and the modified ones are listed below:

$$2D\lambda_\tau = \lambda_\tau \left( - \sum_i C\tau_i (4\pi\alpha_i) + \lambda_b^2 + 4\lambda_\tau^2 + 4f_3^2 \right), \quad (\text{A1})$$

where  $C\tau_i = 9/5, 3, 0$  and  $D \equiv 16\pi^2/2(d/dt)$ ,

$$2Df_3 = f_3 \left( - \sum_i Cf_{3i} (4\pi\alpha_i) + 10f_3^2 + 4\lambda_\tau^2 \right), \quad (\text{A2})$$

where  $Cf_{3i}=36/5,0,0$ ,

$$Dm_{\tau^c}^2 = -\frac{48}{5}\pi\alpha_1\tilde{M}_1^2 + 2\lambda_\tau^2(m_{\tau^c}^2 + m_\tau^2 + M_{H1}^2 + A_\tau^2) + 4f_3^2(m_{\Delta^{\pm\pm}}^2 + 2m_{\tau^c}^2 + A_3^2), \quad (\text{A3})$$

$$Dm_{\Delta^{\pm\pm}}^2 = -\frac{192}{5}\pi\alpha_1\tilde{M}_1^2 + 2f_3^2(m_{\Delta^{\pm\pm}}^2 + 2m_{\tau^c}^2 + A_3^2). \quad (\text{A4})$$

We do not include the effects of the couplings to the other generation  $f_{1,2}$  since they are very small:

$$DA_\tau = \left( \sum_i C\tau_i 4\pi\alpha_i M_i + \lambda_b^2 A_b + 4\lambda_\tau^2 A_\tau + 4f_3^2 A_3 \right), \quad (\text{A5})$$

$$DA_3 = \left( (4\pi\alpha_1)\frac{36}{5}M_1 + 10f_3^2 A_3 + 4\lambda_\tau^2 A_\tau \right), \quad (\text{A6})$$

$$2DM_{\tilde{\Delta}^{\pm\pm}} = M_{\tilde{\Delta}^{\pm\pm}} \left( -(4\pi\alpha_1)\frac{48}{5} + 4f_3^2 \right). \quad (\text{A7})$$

- 
- [1] R. N. Mohapatra, Phys. Rev. D **34**, 3457 (1986); A. Font, L. Ibanez, and F. Quevedo, Phys. Lett. B **228**, 79 (1989); S. Martin, Phys. Rev. D **46**, 2769 (1992).
- [2] R. N. Mohapatra and A. Rasin, Phys. Rev. Lett. **76**, 3490 (1996); R. Kuchimanchi, *ibid.* **76**, 3486 (1996); R. N. Mohapatra, A. Rasin, and G. Senjanović, *ibid.* **79**, 4744 (1997).
- [3] M. Gell-Mann, P. Ramond, and R. Slansky, in *Supergravity*, Proceedings of the Workshop, Stony Brook, New York, 1979, edited by D. Freedman and P. van Nieuwenhuizen (North-Holland, Amsterdam, 1979); T. Yanagida, in *Proceedings of the Workshop on Unified Theories and Baryon Number in the Universe*, Tsukuba, Japan, 1979, edited by O. Sawada and A. Sugamoto (KEK Report No. 79-18, Tsukuba, 1979); R. N. Mohapatra and G. Senjanović, Phys. Rev. Lett. **44**, 912 (1980).
- [4] R. Kuchimanchi and R. N. Mohapatra, Phys. Rev. D **48**, 4352 (1993); Phys. Rev. Lett. **75**, 3989 (1995).
- [5] C. S. Aulakh, A. Melfo, and G. Senjanović, Phys. Rev. D **57**, 4174 (1998); C. S. Aulakh, A. Melfo, A. Rasin, and G. Senjanović, hep-ph/9712551 (unpublished).
- [6] Z. Chacko and R. N. Mohapatra, Phys. Rev. D **58**, 015001 (1998).
- [7] C. S. Aulakh, K. Benakli, and G. Senjanović, Phys. Rev. Lett. **79**, 2188 (1997).
- [8] K. Jungman, invited talk in PASCOS98 (1998).
- [9] M. Dine and A. Nelson, Phys. Rev. D **48**, 1277 (1993); M. Dine, A. E. Nelson, Y. Nir, and Y. Shirman, *ibid.* **53**, 2658 (1996); A. E. Nelson, Prog. Theor. Phys. Suppl. **123**, 365 (1996); M. Dine, A. E. Nelson, and Y. Shirman, Phys. Rev. D **51**, 1362 (1995).
- [10] K. S. Babu, B. Dutta, and R. N. Mohapatra (in preparation).
- [11] Similar ideas in the context of MSSM and other models have been considered earlier by T. Blazek, S. Raby, and S. Pokorski, Phys. Rev. D **52**, 4151 (1995); C. Hamazoui and M. Pospelov, hep-ph/9803354.
- [12] F. Gabbiani, E. Gabrielli, A. Masiero, and L. Sestini, Nucl. Phys. **B477**, 321 (1996).
- [13] R. N. Mohapatra, G. Senjanović, and M. Tran, Phys. Rev. D **28**, 546 (1983); G. Ecker, W. Grimus, and H. Neufeld, Phys. Lett. **127B**, 365 (1983); F. Gilman and M. Reno, Phys. Rev. D **29**, 937 (1983); M. Pospelov, *ibid.* **56**, 259 (1997); G. Barenboim, J. Bernabeu, and M. Raidal, Valencia report, 1996.
- [14] V. Barger, M. S. Berger, and P. Ohmann, Phys. Rev. D **47**, 1093 (1993).
- [15] S. Martin, in *Perspectives in Supersymmetry*, edited by G. Kane (World Scientific, Singapore, 1998), hep-ph/9709356.
- [16] V. Barger, M. Berger, and P. Ohman, Phys. Rev. D **49**, 4908 (1994).
- [17] N. G. Deshpande, B. Dutta, and E. Keith, Phys. Rev. D **54**, 730 (1996).
- [18] R. N. Mohapatra and B. Dutta (work in progress).
- [19] ALEPH Collaboration, Report Nos. ALEPH-98-014, CONF 98-004.
- [20] M. Lusignoli and S. Petrarca, Phys. Lett. B **226**, 397 (1989); K. Huitu, J. Maalampi, and M. Raidal, Nucl. Phys. **B420**, 449 (1994); Phys. Lett. B **320**, 60 (1994); F. Cuyper and S. Davidson, Eur. Phys. J. C **2**, 503 (1998); F. Cuyper and M. Raidal, Nucl. Phys. **B501**, 3 (1997); M. Raidal, Phys. Rev. D **57**, 2013 (1998); K. Huitu, J. Maalampi, A. Pietila, and M. Raidal, Nucl. Phys. **B487**, 27 (1997); J. Gunion, C. Loomis, and K. T. Pitts, hep-ph/9610237; C. Picciotto, Phys. Rev. D **56**, 1612 (1997); S. Chakrabarti, D. Choudhury, R. M. Godbole, and B. Mukhopadhyaya, hep-ph/9804297; for earlier applications of the light doubly charged Higgs bosons of left-right symmetric models, see M. L. Swartz, Phys. Rev. D **40**, 1521 (1989); P. Herczeg and R. N. Mohapatra, Phys. Rev. Lett. **69**, 2475 (1992); A. Halprin, *ibid.* **48**, 1313 (1982); J. Gunion, J. Grifols, B. Kayser, A. Mendez, and F. Olness, Phys. Rev. D **40**, 1546 (1989).
- [21] S. Dimopoulos, S. Thomas, and J. D. Wells, Nucl. Phys. **B488**, 39 (1997); H. Baer, M. Brhlik, C.-H. Chen, and X. Tata, Phys. Rev. D **55**, 4463 (1997); N. G. Deshpande, B. Dutta, and S. Oh, *ibid.* **56**, 519 (1997); R. Rattazzi and Uri Sarid, Nucl. Phys. **B501**, 297 (1997).
- [22] H. Pagels and J. Primack, Phys. Rev. Lett. **48**, 223 (1982).
- [23] ALEPH Collaboration, ALEPH-98-013, CONF 98-003; C. Chang and G. Snow, UMD-PP-98-92.
- [24] D. A. Dicus, B. Dutta, and S. Nandi, Phys. Rev. Lett. **78**, 3055 (1997); F. M. Borzumati, hep-ph/9702307; S. Ambrosanio, G. Kribs, and S. Martin, Phys. Rev. D **56**, 1761 (1997).
- [25] S. Ambrosanio, Graham D. Kribs, and Stephen P. Martin, Nucl. Phys. **B516**, 55 (1998); K. Cheung, D. A. Dicus, B. Dutta, and S. Nandi, Phys. Rev. D **58**, 015008 (1998).